ELSEVIER

Journal of Alloys and Compounds 434–435 (2007) 240–243

Journal of ALLOYS AND COMPOUNDS

www.elsevier.com/locate/jallcom

Formation and corrosion behavior of glassy Ni–Nb–Ti–Zr–Co(–Cu) alloys

S.J. Pang [a,b], C.H. Shek [b], K. Asami [c],
A. Inoue [c], T. Zhang [a,*]

[a] Department of Materials Science and Engineering, Beijing University of Aeronautics and Astronautics, Beijing 100083, China
[b] Department of Physics and Materials Science, City University of Hong Kong, Hong Kong, China
[c] Institute for Materials Research, Tohoku University, Sendai 980-8577, Japan

Abstract

Bulk glassy $Ni_{55}Nb_{20}Ti_{10}Zr_8Co_7$ alloy with a critical diameter of 2 mm was synthesized by copper-mold casting and the glass transition temperature, crystallization temperature and supercooled liquid region are 858 K, 911 K and 52 K, respectively. High corrosion resistance in 1N HCl and H_2SO_4 solutions was recognized for the glassy alloys $Ni_{55}Nb_{20}Ti_{10}Zr_8Co_7$ together with $Ni_{53}Nb_{20}Ti_{10}Zr_8Co_6Cu_3$ which possesses higher glass-forming ability. They are spontaneously passivated with low passive current densities of the order of 10^{-2} A/m^2 and their corrosion rate was less than 10^{-3} mm/year in the solutions. A small amount addition of Cu (3 at.%) in the Ni–Nb–Ti–Zr–Co glassy alloy system has little effect on corrosion behavior and surface film composition. Niobium-rich passive films form on the glassy Ni–Nb–Ti–Zr–Co(–Cu) alloys, which could be responsible for the high corrosion resistance.

Keywords: Amorphous materials; Ni-based alloys; Thermal analysis; Corrosion

1. Introduction

Since the synthesis of $Ni_{53}Nb_{20}Ti_{10}Zr_8Co_6Cu_3$ (at.%) bulk metallic glass (BMG) with high strength of 3000 MPa by copper-mold casting [1], formation of Ni-based BMGs in metal–metal system type has been reported in Ni–Nb–Ti–Zr(–Co), Ni–Ta–Ti–Zr(–Co), Ni–Nb–Ti, Ni–Nb–Ti–Hf, Ni–Cu–Ti–Zr–Al and Ni–Nb–Ti–Pt systems in recent years [2–10]. It is notable that the glassy Ni–Nb–Ti–Zr–Co and Ni–Ta–Ti–Zr–Co alloys, for which the critical diameters for glass-formation (t_{max}) was up to 1.5 mm, possess extremely high corrosion resistance in aggressive acids mainly due to the formation of passive film significantly enriched with Nb or Ta on the alloy surface [3–5,11]. Recently, by a slight adjustment of the alloy composition in Ni–Nb–Ti–Zr–Co system, we found an alloy, $Ni_{55}Nb_{20}Ti_{10}Zr_8Co_7$ (at.%), exhibiting higher glass-forming ability (GFA) and the t_{max} reached 2 mm by copper-mold casting. On the other hand, in the Ni–(Nb, Ta)–Ti–TM (TM = Zr, Hf, Co, Pt) systems, the $Ni_{53}Nb_{20}Ti_{10}Zr_8Co_6Cu_3$ alloy containing a small amount of Cu exhibited the highest GFA as evidenced by its t_{max} of 3 mm [1–8,10], while its corrosion resistance is unknown. It is of scientific and engineering importance to characterize the corrosion behavior of the glassy $Ni_{55}Nb_{20}Ti_{10}Zr_8Co_7$ and $Ni_{53}Nb_{20}Ti_{10}Zr_8Co_6Cu_3$ alloys and the effect of Cu addition on the corrosion resistance. This paper intends to present the thermal stability and GFA of the glassy $Ni_{55}Nb_{20}Ti_{10}Zr_8Co_7$ alloy, and the corrosion behavior and surface film compositions of the glassy $Ni_{55}Nb_{20}Ti_{10}Zr_8Co_7$ and $Ni_{53}Nb_{20}Ti_{10}Zr_8Co_6Cu_3$ alloys in 1N H_2SO_4 and 1N HCl solutions. The effect of Cu addition on corrosion resistance is also discussed.

2. Experimental procedure

Alloy ingots with nominal compositions of $Ni_{55}Nb_{20}Ti_{10}Zr_8Co_7$ and $Ni_{53}Nb_{20}Ti_{10}Zr_8Co_6Cu_3$ (at.%) were prepared by arc melting the mixture of the pure metals in an argon atmosphere. From the ingots, alloy ribbons of about 0.02 mm in thickness and 1 mm in width and cylindrical rods of 2 mm in diameter were produced by melt spinning and copper-mold casting, respectively, in an argon atmosphere. The structure of the samples was examined by X-ray diffraction (XRD) with Cu Kα radiation. The thermal stability associated with

---

[*] Corresponding author. Tel.: +86 1082314869; fax: +86 1082314869.
E-mail address: zhangtao@buaa.edu.cn (T. Zhang).

0925-8388/$ – see front matter © 2006 Elsevier B.V. All rights reserved.
doi:10.1016/j.jallcom.2006.08.289

the glass transition, supercooled liquid region and crystallization of the glassy alloys was investigated by differential scanning calorimetry (DSC) at a heating rate of 0.67 K/s.

Corrosion behavior of the glassy alloys in 1N HCl and 1N H_2SO_4 solutions open to air was characterized by immersion test and electrochemical measurements using the ribbon specimens at room temperature. For comparison, potentiodynamic polarization curves of the pure metals and a stainless steel SUS316L were also measured. Prior to the corrosion tests the specimens were mechanically polished in cyclohexane with silicon carbide paper up to no. 1500, degreased in acetone, dried in air and then further exposed to the laboratory air for 24 h. For estimating the corrosion rates, the weight loss of the glassy alloys after immersion in the solutions for 168 h was measured. Electrochemical measurements were conducted in a three-electrode cell with a platinum counter electrode and a Ag/AgCl reference electrode. Potentiodynamic polarization curves were measured at a potential sweep rate of 50 mV/min after open-circuit immersing the specimens for about 30 min, when the open-circuit potentials became almost steady. The change in open-circuit potential with immersion time was recorded.

The surface of the glassy alloy specimens before and after the immersion tests was analyzed by X-ray photoelectron spectroscopy (XPS). The X-ray photoelectron spectra were measured using a SSI SSX-100 photoelectron spectrometer with monochromatized Al Kα radiation ($h\nu = 1486.6$ eV). The compositions of the surface film and the underlying alloy surface were quantitatively determined from the XPS spectra using a previously proposed method using the integrated intensities of photoelectrons under the assumption of a three layer model [12,13]. The binding energies of the electrons were calibrated by using the method described elsewhere [14,15].

3. Results and discussion

Fig. 1 shows the DSC curve and X-ray diffraction pattern (the inset) of $Ni_{55}Nb_{20}Ti_{10}Zr_8Co_7$ cast rod with its t_{max} of 2 mm together with the DSC trace of the alloy ribbon for comparison. The XRD pattern shows a broad peak associated with a glassy phase and no detectable crystalline peaks. The DSC curves indicate no distinct difference in glass transition temperature (T_g), crystallization temperature (T_x), supercooled liquid region ($\Delta T_x = T_x - T_g$) and heat of crystallization (ΔH_x) between the ribbon and rod samples, further confirming the glassy single phase structure of the bulk sample. The T_g, T_x, ΔT_x and ΔH_x of the glassy $Ni_{55}Nb_{20}Ti_{10}Zr_8Co_7$ alloy are about 858 K, 911 K, 52 K and 4.4 kJ/mol, respectively. It is indicated that the $Ni_{55}Nb_{20}Ti_{10}Zr_8Co_7$ alloy with a critical diameter of 2 mm possesses larger supercooled liquid region and higher GFA than the previously reported Ni–Nb–Ti–Zr–Co alloys, including $Ni_{55}Nb_{20}Ti_{10}Zr_{10}Co_5$ ($t_{max} = 1.5$ mm). This implies that the GFA of the Ni–Nb–Ti–Zr–Co system is sensitive to the composition variation and a slight appropriate adjustment in the composition may improve the GFA. The high thermal stability of supercooled liquid against crystallization for the $Ni_{55}Nb_{20}Ti_{10}Zr_8Co_7$ alloy could facilitate the easier vitrification.

Corrosion behavior of the glassy $Ni_{55}Nb_{20}Ti_{10}Zr_8Co_7$ and $Ni_{53}Nb_{20}Ti_{10}Zr_8Co_6Cu_3$ (its glassy structure was confirmed by XRD and DSC) alloys in 1N HCl and 1N H_2SO_4 solutions was investigated. No weight loss was detected for the two glassy alloys after immersion in the solutions open to air for 1 week, indicating a corrosion rate of less than 10^{-3} mm/year, which was the reproducibility limit of the measurement in this work.

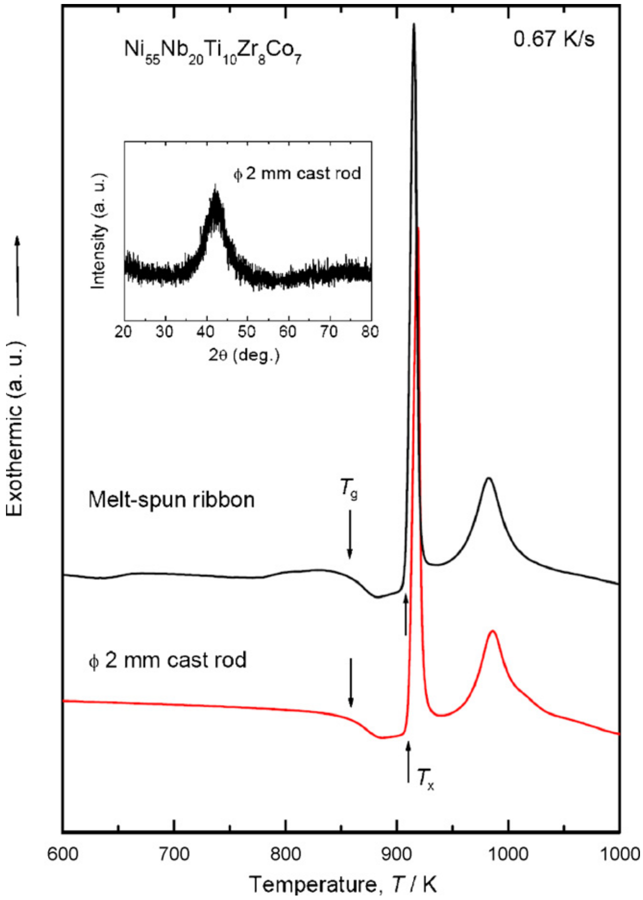

Fig. 1. DSC curves of glassy $Ni_{55}Nb_{20}Ti_{10}Zr_8Co_7$ alloy ribbon and rod with a diameter of 2 mm. The inset shows the XRD pattern of the $Ni_{55}Nb_{20}Ti_{10}Zr_8Co_7$ cast rod.

For a further understanding of the corrosion behavior of the glassy $Ni_{55}Nb_{20}Ti_{10}Zr_8Co_7$ and $Ni_{53}Nb_{20}Ti_{10}Zr_8Co_6Cu_3$ alloys and investigating the effect of Cu addition on the corrosion resistance, the glassy alloys were also characterized by electrochemical measurements in the H_2SO_4 and HCl solutions. The changes in the open-circuit potentials with immersion time in the acids are almost the same for the glassy alloys with and without Cu, as shown in Fig. 2. For both of the alloys, the poten-

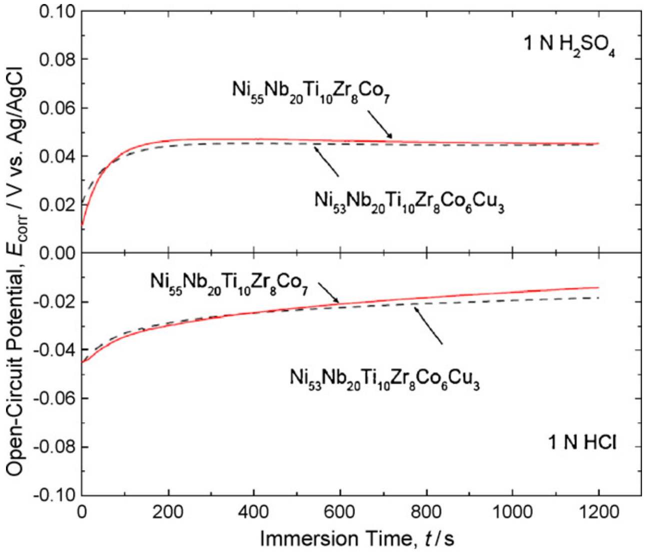

Fig. 2. Change in open-circuit potential with immersion time for the glassy Ni–Nb–Ti–Zr–Co(–Cu) alloys in 1N H_2SO_4 and 1N HCl solutions.

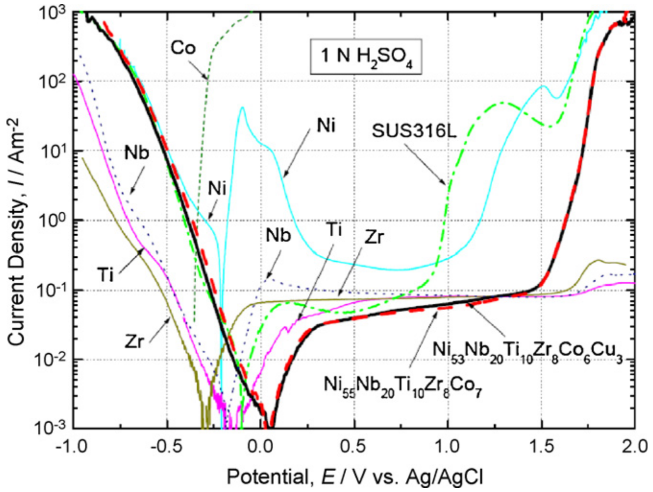

Fig. 3. Potentiodynamic polarization curves of the glassy Ni–Nb–Ti–Zr–Co(–Cu) alloys, pure nickel, niobium, zirconium, titanium and cobalt and SUS316L in 1N H_2SO_4 solution.

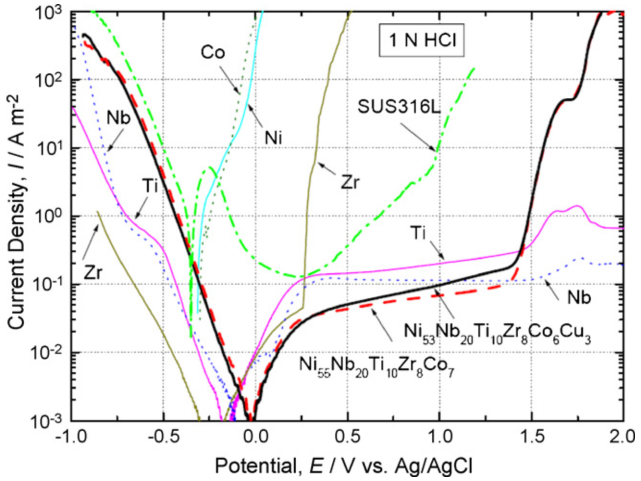

Fig. 4. Potentiodynamic polarization curves of the glassy Ni–Nb–Ti–Zr–Co(–Cu) alloys, pure nickel, niobium, zirconium, titanium and cobalt and SUS316L in 1N HCl solution.

tials initially rise quickly with immersion time and slow down to reach stationary values, indicating the improvement of stability of the surface films during immersion.

Fig. 3 shows the potentiodynamic polarization curves of the glassy $Ni_{55}Nb_{20}Ti_{10}Zr_8Co_7$ and $Ni_{53}Nb_{20}Ti_{10}Zr_8Co_6Cu_3$ alloys, pure Ni, Nb, Ti, Zr, Co and SUS316L in 1N H_2SO_4 solution. Nb, Ti, Zr and SUS316L are spontaneously passivated with low passive current density, while active dissolution occurs by a slight anodic polarization for Ni and Co in the acid. There is no apparent difference in polarization behavior between the two glassy Ni–Nb–Ti–Zr–Co(–Cu) alloys. They are spontaneously passivated with a passive current density of about 3×10^{-2} A/m^2, which is slightly lower than those of the pure metals and SUS316L. The cathodic activity of the alloys are almost the same as that of SUS316L and much higher than those of pure Nb, Ti and Zr. In the potential range higher than 1.5 V, the current density of the glassy alloys increases rapidly with potential, which may correspond to the evolution of O_2.

Polarization curves in 1N HCl solution are shown in Fig. 4. In 1N HCl solution, Nb, Ti and Zr are spontaneously passivated. For pure Zr, pitting corrosion occurs at about 0.25 V, while Co and Ni actively dissolve by the anodic polarization. SUS316L exhibits active dissolution prior to passivation. The glassy alloys are spontaneously passivated with lower passive current densities than those of Nb, Ti, Zr and SUS316L until about 1.2 V. At about 1.35 V, they show abrupt increase in the anodic current because of O_2 and/or Cl_2 gas evolution. It is also recognized that in the HCl solution the passive current density of the Ni–Nb–Ti–Zr–Co–Cu alloy is slightly higher than that of the alloy free-from Cu. The results indicate that the present Ni–Nb–Ti–Zr–Co(–Cu) glassy alloys possess extremely high corrosion resistance in the acids, though the addition of a small amount of Cu in the alloy is slightly detrimental to the corrosion resistance in the aggressive HCl solution. In addition, the corrosion behavior of the present alloys is similar to those of the other glassy Ni–Nb–Ti–Zr–Co and Ni–Ta–Ti–Zr–Co alloys with similar Nb/Ta, Ti and Zr contents [3–5], implying that the alloying elements Nb, Ti and Zr are responsible for the high corrosion resistance. Our previous work has demonstrated that Nb, Ti and Zr are significantly enriched in the surface films on the glassy $Ni_{55}Nb_{20}Ti_{10}Zr_{10}Co_5$ alloy exposed to air and on those immersed in HCl solutions in comparison with the nominal alloy compositions [4,11]. For clarifying the origin of the high corrosion resistance of the glassy alloys in Ni–Nb–Ti–Zr–Co(–Cu) system, the surface films formed in air and in the acids for the glassy $Ni_{55}Nb_{20}Ti_{10}Zr_8Co_7$ and $Ni_{53}Nb_{20}Ti_{10}Zr_8Co_6Cu_3$ alloys were analyzed by XPS.

The XPS spectra of the glassy Ni–Nb–Ti–Zr–Co(–Cu) alloys exhibited peaks of nickel, niobium, titanium, zirconium, cobalt, oxygen and carbon. Copper peaks were also detected for the Cu-containing alloy. The C 1s peaks were those from so-called contaminant carbon on the top surface of the specimen. The O 1s spectrum consisted of peaks originating from oxygen in metal—O—metal bond, metal—OH bond and/or bound water. The peaks of Ni 2p, Co 2p, Nb 3d, Ti 2p, Zr 3d and Cu LMM were composed of peaks corresponding to the species in the oxidized states in a surface film and the metallic states in an underlying alloy surface.

Fig. 5 shows the cationic contents in the surface films for the glassy Ni–Nb–Ti–Zr–Co(–Cu) alloys exposed to air and those immersed in the acids for 1 week. In the surface films formed by air exposure for both of the alloys, Nb, Ti and Zr are enriched, while Ni is deficient in comparison with the nominal alloy compositions. After immersion in the H_2SO_4 and HCl solutions, in the surface films of the two alloys the contents of Nb increase significantly while those of Ni decrease, though no apparent change in the contents of Ti, Zr and Co is recognized. The facts indicate that the air-formed films on the alloys were not stable in the acidic solutions and converted to the passive films in which Nb was further concentrated during the immersion. The formation of Nb-rich passive films could be responsible for the high corrosion resistance of the glassy Ni–Nb–Ti–Zr–Co(–Cu) alloys. Moreover, for the 3 at.% Cu-containing alloy, Cu contents in the surface films formed in air or in the H_2SO_4 solution

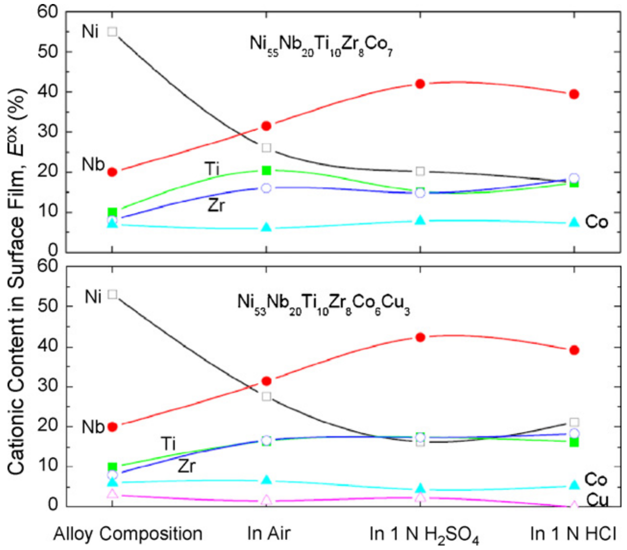

Fig. 5. Cationic contents in the surface films for the glassy Ni–Nb–Ti–Zr–Co(–Cu) alloys exposed to air and those immersed in 1N H_2SO_4 and 1N HCl solutions for 1 week.

are lower than that in the bulk alloy, and no Cu is detected in the surface film formed in the HCl solution. This indicates that Cu in the alloy has little effect on the surface film composition. On the other hand, XPS analysis also indicated that, in the underlying alloy surface of the Cu-containing alloy exposed to air or immersed in the solutions, copper was significantly enriched with concentration in the range of 14.2–22.6 at.%, which is much higher than the nominal Cu content in the alloy. It can be said that when the alloys were exposed to air, Nb, Ti and Zr were preferentially oxidized and resulted in enrichment of these valve-metals in the surface films. By immersion in the solutions, Nb enrichment in the surface film was promoted while unstable Ni dissolved much easier. Thus, stable passive films enriched with the valve-metal cations were formed.

4. Conclusions

(1) Bulk glassy $Ni_{55}Nb_{20}Ti_{10}Zr_8Co_7$ alloy rods up to 2 mm in diameter are able to be synthesized by copper-mold casting. The T_g, T_x and ΔT_x are 858 K, 911 K and 52 K, respectively.
(2) The glassy $Ni_{55}Nb_{20}Ti_{10}Zr_8Co_7$ and $Ni_{53}Nb_{20}Ti_{10}Zr_8Co_6Cu_3$ alloys exhibited high corrosion resistance in 1N HCl and 1N H_2SO_4 solutions. Their corrosion rate was less than 10^{-3} mm/year and they were spontaneously passivated with passive current densities of the order of 10^{-2} A/m^2, lower than those of the pure valve-metals and SUS316 in a certain large potential range.
(3) In the HCl and H_2SO_4 solutions, there is no apparent difference in corrosion behavior and surface film composition between the glassy alloys containing and free-from Cu.
(4) Nb, Ti and Zr are enriched while Ni is deficient in the surface film in comparison with the nominal alloy compositions for the glassy Ni–Nb–Ti–Zr–Co(–Cu) alloys exposed to air and those immersed in the acids.
(5) The high corrosion resistance is attributed to the formation of a niobium-rich passive films on the alloys by air-exposure and immersion in the solutions.

Acknowledgements

S.J. Pang would like to acknowledge the financial support by the Young Scholars Scheme of the Faculty of Science and Engineering, City University of Hong Kong. Thanks are also due to the support of the National Natural Science Foundation of China (Nos. 50225103 and 50471001).

References

[1] T. Zhang, A. Inoue, Mater. Trans. 43 (2002) 708.
[2] A. Inoue, W. Zhang, T. Zhang, Mater. Trans. 43 (2002) 1952.
[3] S.J. Pang, T. Zhang, K. Asami, A. Inoue, Mater. Trans. 43 (2002) 1771.
[4] S.J. Pang, T. Zhang, K. Asami, A. Inoue, Mater. Sci. Eng. A 375–377 (2004) 368.
[5] T. Zhang, S.J. Pang, K. Asami, A. Inoue, Mater. Trans. 44 (2003) 2322.
[6] W. Zhang, A. Inoue, Mater. Trans. 43 (2002) 2342.
[7] W. Zhang, A. Inoue, Scripta Mater. 48 (2003) 641.
[8] A. Inoue, W. Zhang, T. Zhang, K. Kurosaka, D.V. Louzguine, J. Metastable Nanocryst. Mater. 15–16 (2003) 3.
[9] D. Xu, G. Duan, W.L. Johnson, C. Garland, Acta Mater. 52 (2004) 3493.
[10] T. Shimada, D.V. Louzguine, J. Saida, A. Inoue, Mater. Trans. 46 (2005) 675.
[11] S.J. Pang, C.H. Shek, T. Zhang, K. Asami, A. Inoue, Corros. Sci. 48 (2006) 625.
[12] K. Asami, K. Hashimoto, S. Shimodaira, Corros. Sci. 17 (1977) 713.
[13] K. Asami, K. Hashimoto, Corros. Sci. 24 (1984) 83.
[14] K. Asami, J. Electron. Spectrosc. 9 (1976) 469.
[15] K. Asami, K. Hashimoto, Corros. Sci. 17 (1977) 559.